Industrial grade $LaCe_{1.85}Pr_{0.03}Nd_{0.06}O_x/Na_2CO_3$ nanocomposite for novel low-temperature semiconductor-ionic membrane fuel cell

Yanyan Liu[1], Wei Zhang[2], Baoyuan Wang[2], Muhammad Afzal[1], Chen Xia[1], Bin Zhu[1, 2]*

[1]*Department of Energy Technology, KTH Royal Institute of Technology, Stockholm, SE-10044, Sweden*
[2]*Hubei Collaborative Innovation Center for Advanced Organic Chemical Materials, Faculty of Physics and Electronic Science, Hubei University, Wuhan, Hubei 430062, P.R. China*

*Corresponding author. E-mail: binzhu@kth.se

Received: 30 September 2016, Revised: 23 October 2016 and Accepted: 20 November 2016

DOI: 10.5185/amlett.2017.7052
www.vbripress.com/aml

Abstract

Doped ceria electrolytes have attracted intensive attentions owing to their high ionic conductivity, low activation energy, good catalytic activity and feasibility for intermediate or even low temperature operations. This work reports an interesting industrial grade rare earth $LaCe_{1.85}Pr_{0.03}Nd_{0.06}$-oxide composited with sodium carbonate (LCPN-oxide/Na_2CO_3) as the electrolyte in solid oxide fuel cells (SOFCs). The 'symmetrical' anode/electrolyte/cathode SOFC devices are fabricated using LCPN-oxide/Na_2CO_3 electrolyte and the lithiated transition metal oxide $Ni_{0.8}Co_{0.15}Al_{0.05}LiO_2$ (NCAL) pasted onto nickel foam as both anode and cathode. A power density of 362 mW/cm^2 is achieved at 550 ^{o}C for this device. A novel fuel cell device, semiconductor-ionic membrane fuel cell (SIMFC) is introduced here using the LCPN-oxide/Na_2CO_3 and NCAL as the mixed semiconductor-ionic conductor layer. The peak power density for this new energy conversion device reaches 916 mW/cm^2 at 550 ^{o}C with an open circuit voltage of 1.05 V. The results demonstrate that industrial grade LCPN-oxide/Na_2CO_3 can provide a new approach to utilize the enriched natural resources for next-generation cost-effective fuel cells.

Keywords: LT-SOFCs, SIMFCs, industrial grade, LCPN-oxide/Na_2CO_3.

Introduction

Solid oxide fuel cells (SOFCs) as potential electrochemical energy conversion devices have been considered to perform several other categories of fuel cell devices based on different conducting electrolyte, feeding fuel or operating temperature in terms of energy efficiency, exhaust heat and fuel flexibility [**1**]. Conventional fuel cells, comprising of anode, electrolyte and cathode, are often limited to develop for commercialization due to the property of electrolyte, e.g. the ionic conductivity of the electrolyte far below 0.1 S cm at low operating temperature (below 600 ^{o}C), and production cost [**2**]. For instance, yttrium stabilized zirconia (YSZ), a dominant SOFC electrolyte, can reach up to 0.1 S/cm at high operation temperature 900-1000 ^{o}C. Many efforts have been contributed to improve the conductive capacity of electrolyte for low operation temperature and reduce the cost to realize commercialization of SOFC technology.

The fluorite structure ceria-based electrolyte materials, have attracted intensive attention due to their improved ionic conductivity, high catalytic activity and lower activation energy for low temperature SOFCs (LT-SOFCs) [**3**, **4**]. The main strength of ceria-based oxide is to extend the high temperature SOFCs to an intermediate or low temperature range (500-600 ^{o}C) with good compatibility with electrodes. Doping with lower valence metal cations is an efficient approach to introduce oxide vacancies and induce the high ionic conductivity of ceria by chemical defects or charge compensation [**5**]. So far, some typical substitutes of Ce^{4+} doped materials have obtained significant achievements for LT-SOFCs from ionic conductivity aspect, such as $Ce_{0.8}Sm_{0.2}O_{1.9}$ (SDC) and $Ce_{0.8}Gd_{0.2}O_{1.9}$ (GDC). Recently, an increasing interest of Pr or/and Nd doped ceria electrolyte materials are developed by improving both ionic conductivity and electrocatalyst functions for high performance LT-SOFC materials. However, a critical issue with the doped ceria oxides is the redox instability induced by the reduction of Ce^{4+} to Ce^{3+} in reducing environment, resulting into electronic conduction and undesirable structural change [**6**].

Major efforts have been attempted to overcome the electronic conductivity of ceria-based electrolytes and improve the ionic conductivity to achieve desired performance at low operation temperature. Virkar *et al.*

[**7**]. utilized YSZ as the electron blocking layer to prevent the electronic leakage current for ceria electrolyte. Hou *et al.* [**8**] developed ceria-bismuth bilayer structured film via a facile method combining co-pressing with drop-coating, which obtained good performance for LT-SOFCs. Naonotechnology approach applied for improving the stability and ionic conductivity of ceria-based oxide has harvested much success. Our pioneer colleagues have also made great contribution to this, especially proposed the concept of nanocomposite and developed pioneer ceria-based nanocomposite materials and technology for advanced LT-SOFCs [**9**, **10**].

Recently, a new fuel-to-electricity conversion device based on ionic-semiconductor materials, as a breakthrough, has been reported in fuel cell technology field [**11-13**]. We construct the semiconductor-ionic membrane fuel cell (SIMFC) by using just a functional ionic-semiconductor layer without an electrolyte separator to realize the fuel cell reactions. The homogenous single layer can integrate the anode, electrolyte and cathode into one component and simplify the fuel cell technology at low manufacturing cost. In this device, the junction structure can be constructed, instead of an ionic electrolyte to block the electron in conventional three-component fuel cell, to eliminate the short-circuiting problem in the new devices. Following this field, we further develop the industrial grade rare-earth lanthanide nitrate LCPN-oxide/Na_2CO_3 nanocomposite in this work via a simple template-free wet chemical synthetic route and its semiconductor-ionic composite approach for this new LT-SOFCs technology at low cost.

Experimental

Material synthesis

$LaCe_{1.85}Pr_{0.03}Nd_{0.06}$-oxide/$Na_2CO_3$ composite nano-crystalline powder (LCPN-oxide/Na_2CO_3) was prepared primarily using the industrial grade rare-earth nitrate via co-precipitation process with sodium carbonate as the precipitating agent to get the rare-earth carbonate precursor in one step. Briefly, industrial grade rare-earth metal nitrates mixture, confirmed with the mass ratio compositions of 63% $Ce(NO_3)_3.6H_2O$, 34% $La(NO_3)_3.6H_2O$, 1% $Pr(NO_3)_3.6H_2O$, 2% $Nd(NO_3)_3.6H_2O$ and negligible amounts of iron and calcium salts were dissolved into deionized water in a beaker as the precursor solution. Carbonate suspension was obtained by adding 2.0 M sodium carbonate solution drop by drop into the beaker until pH value of the solution reached up to 11 and maintaining the vigorous stirring for 2 h at room temperature. Subsequently, the obtained mixture was transferred into the oven and calcined at 750 ^oC for 2 h followed by filtration washing. Then, the obtained powder was suspended in 2 M Na_2CO_3 solution under continuously stirring with Na_2CO_3 weight ratio of 20 wt % of LCPN-oxide. The slurry was dried at 120^oC for 12 h, then a calcination process at 750^oC for 2 h was conducted to obtain the LCPN-oxide/Na_2CO_3 nanocomposite. $Ni_{0.8}Co_{0.85}Al_{0.05}LiO_2$ **(**NCAL**)** was purchased from Tianjin Baomo Joint Hi-Tech venture, China.

Fuel cell fabrication

For the fabrication of 'symmetrical' anode/ electrolyte/cathode fuel cell, the commercial NCAL powder was primarily mixed into terpineol-based slurries to form a slurry; then the NCAL slurry was pasted on nickel foam to function as anode and cathode. The fuel cell devices were constructed by a dry-pressing procedure involving the model with the electrolyte LCPN-oxide/Na_2CO_3 composite powder sandwiched between two NCAL-electrodes pressed under 300 MPa to from a disk fuel cell. The fuel cell was 13 mm in diameter and 1.0 mm with a LCPN-oxide/Na_2CO_3 electrolyte 0.5 mm in thickness. The active area of this device is 0.64 cm^2. The configuration can be noted as Ni (foam) -NCAL | LCPN-oxide/Na_2CO_3 | NCAL-Ni (foam) (Type I), in which nickel foam played a role as current collector and structural support. Hydrogen at a flow rate of 120 ml/min and air at a flow rate of 120-150 ml/min under a pressure of 1 bar were supplied as fuel and oxidant to operate the fuel cell for electrochemical measurements.

Novel cell configuration was fabricated using the as-prepared LCPN-oxide/Na_2CO_3 composite and commercial semiconductor NCAL in volume ratio of 1:1 as semiconductor-ionic membrane layer to replace the LCPN-oxide/Na_2CO_3 electrolyte. The cell configuration is Ni (foam) -NCAL | LCPN-oxide/Na_2CO_3+NCAL (in volume ratio of 1:1) | NCAL-Ni (foam) (Type II).

Materials characterizations

The structure and phase of the as-synthesized material was analyzed using X-ray diffraction (XRD, D-max-2500 X-ray diffractometer, Rigaku Corp., Japan) with filtered Cu Kα radiation. The data were recorded in a step-scan mode of the 2theta range of 10-80^o with step size 0.02^o. Scanning electron microscopy (SEM) was performed on a cold field emission scanning electron microscope (Hitachi S-4800).

Electrochemical test

The electrochemical performance of fuel cells was measured using a programmable electronic load (ITECH8511, ITECH Electrical Co., Ltd.) at operation temperature 550 ^oC. Electrochemical impedance spectroscopy (EIS) was carried out to evaluate the above two types of fuel cell processes at 550 ^oC upon cooling using an electrochemical workstation (Gamry Reference 3000, USA). The frequency of the EIS measurement ranges from 0.01 Hz to 1.0 Hz with a bias voltage of 10 mV.

Results and discussion

Basic properties

The major components of the industrial grade natural material are determined directly by the heat-treatment of the rare-earth nitrate mixture of La, Ce, Pr and Nd to form

the rare-earth oxides, including CeO_2, La_2O_3, Nd_2O_3 and Pr_6O_{11}. The corresponding mass ratios for the several oxides are shown in **Table 1**.

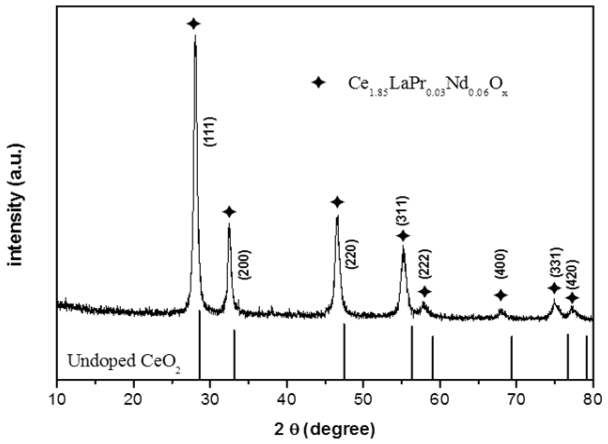

Fig. 1. XRD patterns of LCPN-oxide/Na_2CO_3.

The X-ray diffraction (XRD) patterns of the as-prepared LCPN-oxide/Na_2CO_3 composite powder is displayed in **Fig. 1**. All the diffraction peaks can be indexed to the cubic fluorite-type structure, and no other diffraction peaks are detected. Some amorphous background, indicates the existence of amorphous Na_2CO_3 phase commonly observed in ceria-carbonate composite. The X-ray reflections of the as-synthesized doped-ceria exhibits the evident nanocrystalline nature. The reflections for undoped ceria, according to JCPDS (card no. 34-0394), are presented for a comparison with the XRD patterns. Diffraction peaks of LCPN-oxide/Na_2CO_3 composite are shifted to lower Bragg angles compared with undoped CeO_2, which means that by introducing elements with bigger ionic radii, e.g. La^{3+}, Pr^{3+} and Nd^{3+}, into the ceria lattice leads to the slight lattice expansion. No diffractions are detected for La_2O_3, Pr_6O_{11} and Nd_2O_3, which verifies that all these ions formed the single phase nanocrystalline. The lattice constant of the LCPN-oxide/Na_2CO_3 composite is calculated as 5.411 Å. The crystallite sizes of LCPN-oxide/Na_2CO_3 is calculated per Scherrer's equation:

$$D = K\lambda/(\beta \cos\theta) \quad (1)$$

where, λ represents the wave length of X-rays, β is the half width of diffraction peaks, θ represents the strongest Bragg angle corresponding to (111) plane for all the composites and K is constant value as 0.89. The crystallite size, D, of as-prepared material is approximately 17 nm.

Table 1. Composition for industrial grade rare-earth nitrate by direct heat-treatment.

Sample	CeO_2	La_2O_3	Pr_6O_{11}	Nd_2O_3	Fe_2O_3	CaO
$Re(NO_3)_3$/ wt. %	63	34	1	2	0.005	0.02

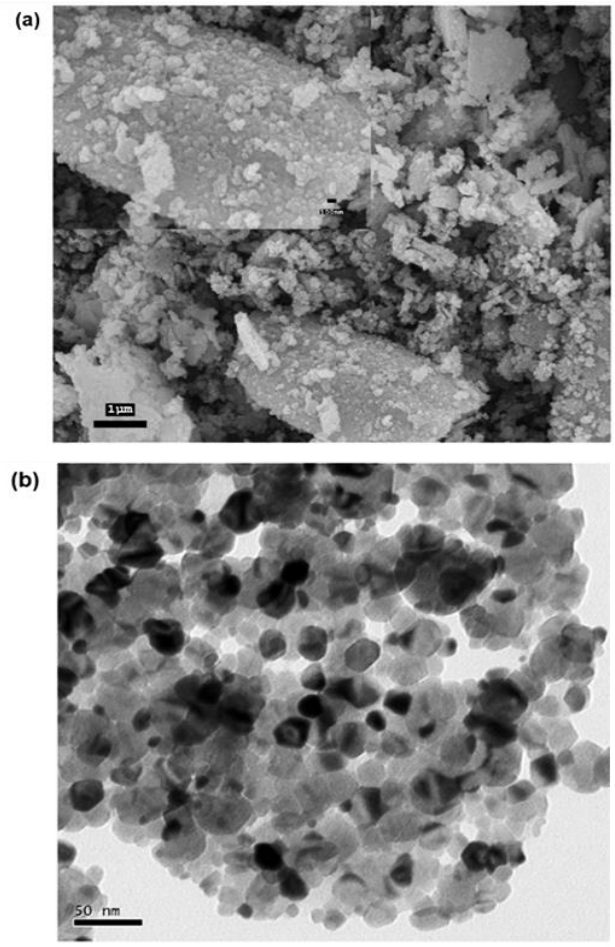

Fig. 2. (a) SEM and (b) TEM images for LCPN-oxide/Na_2CO_3.

Fig. 2 presents the scanning electron microscope (SEM) and transmission electron microscope (TEM) micrographs of as-prepared LCPN-oxide/Na_2CO_3 powder material. The images show that the particle sizes of the LCPN-oxide/Na_2CO_3 mainly distribute around 10-30 nm, which is in agreement with the results from XRD analysis by using Scherrer equation. However, some distinct bulk agglomeration with non-uniform size are also observed in the SEM image since this material is formed at industrial grade.

Electrochemical properties

Fig. 3 shows the impedance spectrum (EIS) measurements for the conventional LCPN/Na_2CO_3 electrolyte fuel cell (Type I) and the SIMFC device (Type II) in FC conditions at 550 °C. The spectra for the two types of devices display the same feature with a semicircle followed by a gradually disappearing tail. To further analyze the detailed kinetic processes for the fuel cell reactions, the equivalent circuit model $R_o/R_1(Q_1)/R_2(Q_2)$ is used to fit the measured data. R_o is from the electrolyte or semiconductor-ionic conductor membrane, electrodes and the connection wires. (R_1-Q_1) and (R_2-Q_2) corresponding to the high and intermediate frequency arcs, respectively [**14**, **15**]. Based on above simulation, the entire resistance of the LCPN-

oxide/Na_2CO_3 or LCPN-oxide/Na_2CO_3-NCAL is equal to $R_{bulk}=R_o+R_1$. The fitted results are summarized in **Table 2**.

Table 2. EIS parameters for equivalent circuits of the two types of devices in FC conditions.

Cell	R_o (ohm cm^2)	R_1 (ohm cm^2)	Q_1 (F cm^{-2})	R_2 (ohm cm^2)	Q_2 (F cm^{-2})
Type I	0.762	1.81	4.19E-05	0.3307	0.3481
Type II	0.764	0.03761	0.00572	2.352	5.34E-02

From the data listed, we can see that the R_1, interphase or grain boundary resistance has been greatly reduced by introducing semiconductor NCAL. More than one order of magnitude is observed, see **Fig. 3** and **Table 2**. It is a possible explanation that the interfaces between the semiconducting and ionic phases in SIMFC device play a vital role to determine the material entire resistance and prove the interfacial conducting mechanism.

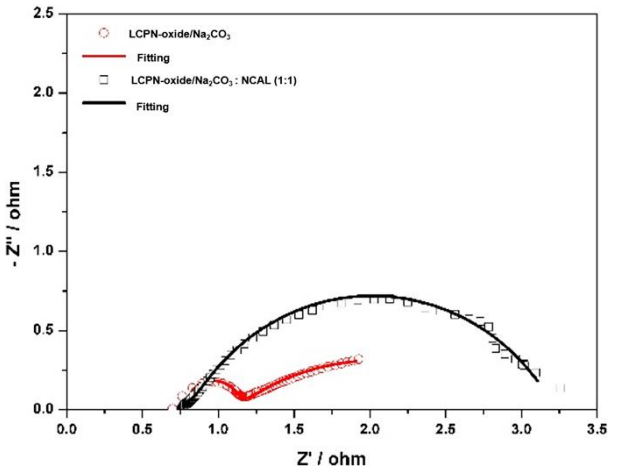

Fig. 3. Impedance spectra for LCPN-oxide/Na_2CO_3 and LCPN-oxide/Na_2CO_3+NCAL (in volume ratio of 1:1) measured in FC condition at 550 °C.

'Symmetrical' anode / electrolyte / cathode SOFC performance

Based on the above EIS results analysis, the LCPN-oxide/Na_2CO_3 nanocomposite is an excellent candidate for the electrolyte of traditional anode/electrolyte/cathode SOFC. **Fig. 4** presents the fuel cell performance of LCPN-oxide/Na_2CO_3 SOFC device with typical current density-voltage (I-V) curve and current density-power density (I-P) characteristics. The fuel cell using the LCPN-oxide/Na_2CO_3 nanocomposite as the electrolyte exhibits high peak power density of 362 mW/cm^2 at 550 °C. The open circuit voltage (OCV) for LCPN-oxide/Na_2CO_3 electrolyte SOFC reaches to 1.0 V, which demonstrates that the commercial NCAL is a good electrocatalyst for anode and cathode reactions. On the other hand, the good OCV of 1.0 V demonstrates that the LCPN-oxide/Na_2CO_3 nanocomposite, as the electrolyte layer, also shows good gas tightness to prevent the gas molecules directly penetrated through the device. This may be attributed to the function of softening amorphous sodium carbonate expanding in the LCPN-oxide network to prevent the gas leakage under the fuel cell operation temperature. It is worth noting that NCAL pasted on the porous nickel foam with good adhesiveness and penetration into nickel foam which can promote the anode and cathode catalyst and kinetic functions. On the other hand, LCPN-based nanocomposites, with plenty of interfaces in the composite, improve the grain-boundary conductivity through increasing the concentration of mobile defects in the space-charge zone, resulting in enhanced ionic conductivity compared with the structural bulk conduction materials. These result in, therefore, a sufficient current output of 1425 mA/cm^2 for LCPN-oxide/Na_2CO_3 nanocomposite electrolyte fuel cell. It can be attributed to the grain-boundary/interface conduction by Nano structuring in both NCAL-Ni electrode and the LCPN-oxide composite electrolyte [**9**, **16**].

It is well known that NiO is a typical p-type semiconductor, due to which the conductivity can be enhanced significantly by doping with various mental ions, such as Li^+. The improved capacity to transfer the ions of doped NiO benefits from increasing the defect concentration in structure [**17**]. The representative semiconductors, e.g. Lithiated NiO (LiNiO), LiNiZn-oxide and LiNiCuSr-oxide composites with ceria, have been successfully developed as new functional semiconductor-ionic materials, applied for the homogenous single layer fuel cells (SLFCs). Their good anode and cathode catalytic functions also have been extensively studied. Besides, NCAL family material, $LiNi_{0.8}Co_{0.2}O_2$ (NCL) has been reported with triple ($H^+/O^{2-}/e^-$) conducting properties for advanced LTSOFC cathode [**17**]. Therefore, the NCAL has shown good 'symmetrical' anode and cathode functions for LCPN-composite electrolyte fuel cells. We further develop the LCPN-oxide/Na_2CO_3 composite by incorporating NCAL semiconductor for novel semiconductor-ionic membrane fuel cells (SIMFCs).

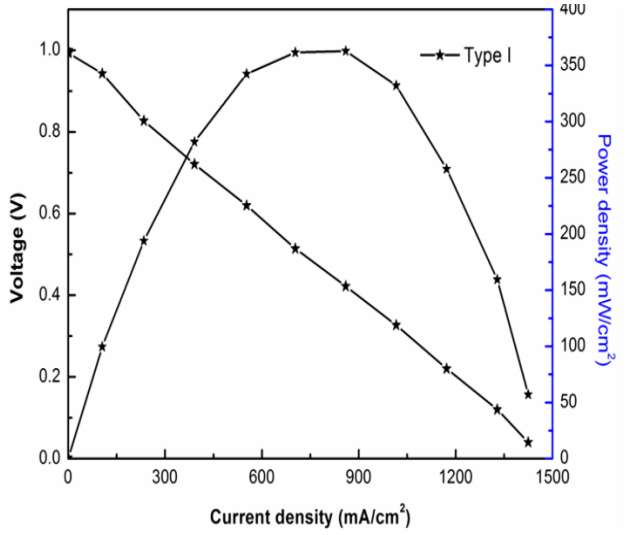

Fig. 4. I-V and I-P characteristics of Ni (foam) -NCAL | LCPN-oxide/Na_2CO_3 | NCAL-Ni (foam) (Type I) at 550 °C.

SIMFC performance

Fig. 5 displays typical I-V and I-P characteristics for SIMFC device using the LCPN-oxide/Na_2CO_3-NCAL composite membrane at various temperature. It is readily distinguished that the SIMFC device exhibits unexceptional electrochemical performance with the maximum power density of 916 mW/cm^2, which is two times greater than that of the conventional LCPN-oxide/Na_2CO_3 electrolyte fuel cell for 362 mW/cm^2. The peak power densities of 423, 540 and 611 mW/cm^2 are achieved corresponding to maximum current densities are 1800, 2104 and 2360 mA/cm^2 at 500ºC, 510ºC and 525ºC, respectively. The significantly enhanced performances have comparability with the previous reports on the doped-ceria electrolyte SOFCs, as the summary in **Table S1** in the supplementary information file **[18-22]**. These improvements on the fuel cell performance can be ascribed to the key component semiconductor and ionic conductor membrane in SIMFC device. The large number of interfaces between the semiconductor and ionic materials can greatly enhance ionic conductivity thus the device current and power outputs are improved. This has been concluded from above EIS analysis.

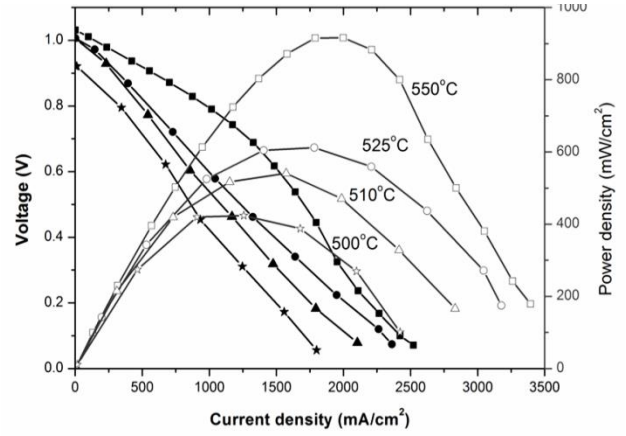

Fig. 5. I-V and I-P characteristics of Ni (foam) -NCAL | LCPN-oxide/Na_2CO_3+NCAL (in volume ratio of 1:1) | NCAL-Ni (foam) (Type II) measured at 500 ºC, 510 ºC, 525 ºC and 550 ºC.

Moreover, the triple ($H^+/O^{2-}/e^-$) conducting properties from the NCAL and good electrocatalyst for hydrogen oxidation and oxygen reduction reactions can lead to excellent SIMFC performances. The results have confirmed that such SIMFC devices can deliver the best energy transfer function. It should be noticed that in the conventional anode/electrolyte/cathode structure, the ionic electrolyte layer separating the anode and cathode does not allow the electronic transport, thus avoids the device short circuiting problem by blocking the electronic passing internally. In the SIMFC structure, we use the 50 vol% NCAL to 50 vol% LCPN-oxide/Na_2CO_3, where NCAL forms percolating electronic conducting paths over the device, but causes no electronic short circuiting problem. It is amazing and hard to be understood by the conventional ion-electrolyte based fuel cell science and technology. As reported previously, the formation of Schottky junction is an essential prerequisite to prevent the electronic short circuit instead of using the electrolyte for electronic blocking layer. In the H_2-contact side, the NCAL surface can be reduced to form a thin NiCo-metal layer to build the Schottky junction with the bulk NCAL, a p-type semiconductor, in the SIMFC membrane. The Schottky junction can block the electrons passing, thus prevent the device from the short circuiting problem. In the latest development, the scientific principle was proposed based on the semiconductor energy bands and junction properties in analogy to the perovskite solar cell work mechanism. The junction structures can avoid the short-circuit problem in the new device, which has the same functionalities as the core component, e.g. hybrid organic-inorganic perovskite, to provide the charge separation in the perovskite solar cell. The authors proposed that the physical properties of the junction combining with the theory of semiconductor energy band can eliminate internal electronic short-circuiting and allow the ion transport in this device [**11**]. On the other hand, the build-in field of the Schottky junction directs to promote the H^+/O^{2-} transfer crossing the metal/semiconductor interface and promote the fuel cell reaction processes thus improve the fuel cell performance. The Schottky junction is associated with the charge transfer processes for H^+/O^{2-} ions in analogy to the ionic conducting electrolyte in conventional fuel cells to implement the fuel cell process. The molecular hydrogen is dissociated into protons in the anode region and the molecular oxygen is reduced into O^{2-} ions in the air input side. The Schottky junction field built in the metal-semiconductor interface, as a driving force, can drive the H^+/O^{2-} ions mobility and assist the conversion from the fuel into electricity [**12**, **23**].

Conclusion

In this work, LCPN-oxide/Na_2CO_3 nanocomposite is successfully synthesized using industrial grade raw material. The conventional LT-SOFC and new SIMFC devices have been developed based on the as-prepared LCPN-oxide/Na_2CO_3 nanocomposite. A maximum power density of 916 mW/cm^2 has been achieved at 550 ºC for the new LCPN-oxide/Na_2CO_3-NCAL SIMFC device, while the conventional LCPN-oxide/Na_2CO_3 electrolyte SOFC reaches only 425 mW/cm^2 at 550 ºC. The enhanced electrochemical performance is analyzed by EIS. The results demonstrate the NCAL semiconductor can significantly reduce the interphase/grain boundary resistance to enhance the ionic conductivity due to interfacial conduction mechanism. The Schottky junction effect has been explored in the NCAL- LCPN-oxide/Na_2CO_3 SIMFC to prevent the internal short-circuiting with excellent performances.

Acknowledgements

This work was supported by the National Science Foundation of China (NSFC, Grant Nos. 51502084), the Natural Science

Foundation of Hubei Province, major project grant No.2015CFA120, the Swedish Research Council (Grant No.621-2011-4983) and the European Commission FP7 TriSOFC-project (Grant No.303454). Authors acknowledge the support of China Scholarship Council for the PhD fellowship.

Author's contributions

Conceived the plan: BZ, YYL; Performed the expeirments: YYL, WZ, BYW; Data analysis: YYL, BZ; Wrote the paper: YYL, BZ, MA, CX. Authors have no competing financial interests.

References

1. Farrell, B., Linic, S. ; *Appl. Catal. B: Environ.*, **2016**, 183: 386. **DOI:**10.1016/j.apcatb.2015.11.002
2. Goodenough J. B.; *Nature*, **2000**, 404, 821. **DOI:**10.1038/35009177
3. Gan, Y., Cheng, J., Li, M., Zhan, H., Sun, W.; *Mater. Chem. Phys.*, **2015**, 163, 279. **DOI:**10.1016/j.matchemphys.2015.07.041
4. Sun, C., Li, H., Chen, L.; *Energy Environ. Sci.*, **2012**, 5, 8475. **DOI:**10.1039/C2EE22310D
5. Marrocchelli, D., Bishop, S. R., Tuller, H. L., Yildiz, B.; *Adv. Funct. Mater.*, **2012**, 22, 1958. **DOI:**10.1002/adfm.201102648
6. Ge, X. M., Chan, S. H., Liu, Q. L., Sun, Q.; *Adv. Energy Mater*. **2012**, 2, 1156. **DOI:**10.1002/aenm.201200342
7. Virkar, A. V.; *J. Electrochem. Soc.*, **1991**, 138, 1481. **DOI:**10.1149/1.2085811
8. Hou, J., Bi, L., Qian, J., Zhu, Z., Zhang, J., Liu, W.; *J. Mater. Chem. A*, **2015**, 3, 10219. **DOI:**10.1039/C4TA06864E
9. Ma, Y., Wang, X., Li, S., Toprak, M. S., Zhu, B., Muhammed, M.; *Adv. Mater*., **2010**, 22, 1640. **DOI:**10.1002/adma.200903402
10. Zhu, B., Fan, L., Lund, P.; *Appl. Energy*, **2013**, 106, 163. **DOI:**10.1016/j.apenergy.2013.01.014
11. Zhu, B., Huang, Y., Fan, L., Ma, Y., Wang, B., Xia, C., Afzal, M., Zhang, B., Dong, W., Wang, H., Lund, P.; *Nano Energy*, **2016**, 19, 156. **DOI:**10.1016/j.nanoen.2015.11.015
12. Zhu, B., Lund, P. D., Raza, R.; Ma, Y., Fan, L. D., Afzal, M., Patakangas, J., Hw, Y. J., Zhao, Y. F., Huang, Q. A., Zhang, J., Wang, H.; *Adv. Energy Mater*., **2015**, 5, 1401895. **DOI:** 10.1002/aenm.201401895
13. Zhu, B., Raza, R., Qin, H., Liu, Q, Fan, L.; *Energy Environ. Sci.*, **2011**, 4, 2986. **DOI:** 10.1039/c1ee01202a
14. Fu, C. J., Sun, K. N., Zhang, N. Q., Chen, X. B., Zhou, D. R.; *Electrochem. Acta*, **2007**, 52, 4589. **DOI:**10.1016/j.electacta.2007.01.001
15. Jespersen, J. L., Tønnesen, A. E., Nørregaard, K., Overgaard, L., Elefsen, F.; *World Electric Vehicle Journal* Vol., 3, **2009**.
16. Wang, X. D., Ma, Y., Raza, R., Muhammed, M., Zhu, B.; *Electrochem. Commun*., **2008**, 10, 1617. **DOI:**10.1016/j.elecom.2008.08.023
17. Fan, L., Su, P. C.; *J. Power Sources*, **2016**, 306, 369. **DOI:**10.1016/j.jpowsour.2015.12.015
18. Sun, W, Liu, W.; *J. Power Sources*, **2012**, 217, 114. **DOI:** 10.1016/j.jpowsour.2012.05.065
19. Courtin, E., Bo, P., Piquero, T., Vulliet, J., Poirot, N., Laberty-Robert, C., *J. Power Sources*, **2012**, 206,77. **DOI:** 10.1016/j.jpowsour.2012.01.109
20. Park, T., Cho, G.Y., Lee, Y. H., Tanveer, W. H., Yu, W., Lee, Y., Kim, Y., An, J., Cha, S.W.; *Int. J. Hydrogen Energy*, **2016**, 41, 9638. **DOI:** 10.1016/j.ijhydene.2016.04.092
21. Sun, H., Zhang, Y., Gong, H., Li, Q., Bu, Y., Li, T..; *Ceram Int*, **2016**, 42, 4285. **DOI:** 10.1016/j.ceramint.2015.11.105
22. Mukai, T., Fujita, T., Tsukui, S., Yoshida, K., Adachi, M., Iwai, H., Takahashi, Y., Goretta, K. C.; *ECS Transactions*, **2015**, 64, 1. **DOI:** 10.1149/06445.0001ecst
23. Hu, H., Lin, Q., Zhu, Z., Liu, X., Afzal, M., He, Y., Zhu, B.; *J. Power Sources*, **2015**, 275, 476. **DOI:** 10.1016/j.jpowsour.2014.11.041

Supplementary information

Table S1. SOFC performance comparison.

No	Device configuration	Performance/ mW/cm^2 (the maximum power output)	Temperature	Article	year
1	Ni-NCAL/LCPN-NCAL/Ni-NCAL	916	550 ºC	-	-
2	Ni-BZCY/SDC/SSC-SDC	511	600 ºC	A novel ceria-based solid oxide fuel cell free from internal short circuit	2012
3	YSZ-NiO/YSZ/YSZ-LSM	350	850 ºC	A composite sol-gel process to prepare a YSZ electrolyte for solid oxide fuel cells	2012
4	Porous Pt/YSZ/Pt	194	500 ºC	Effect of anode morphology on the performance of thin film solid oxide fuel cell with PEALD YSZ electrolyte	2016
5	SDC-NiO/SDC/SDC-SSC	860	650 ºC	Anode-supported SOFCs based on $Sm_{0.2}Ce_{0.8}O_{2-\delta}$ electrolyte thin-films fabricated by co-pressing using microwave combustion synthesized powders	2015
6	NiO-YSZ/YSZ/GDC/LSC/ LSCF	530	600 ºC	Improvement of Thermal reliability and power density of SOFCs by preparing nano LSC particles between GDC electrolyte and LSCF cathode	2015